IOP PUBLISHING PHYSICS IN MEDICINE AND BIOLOGY

Phys. Med. Biol. **54** (2009) 2769–2777 doi:10.1088/0031-9155/54/9/012

Imaging of mesoscopic-scale organisms using selective-plane optoacoustic tomography

Daniel Razansky[1,2,3,5], **Claudio Vinegoni**[3,4] **and Vasilis Ntziachristos**[1,2,3]

[1] Institute for Biological and Medical Imaging, Helmholtz Zentrum München, Ingolstädter Landstraße 1, D-85764 Neuherberg, Germany
[2] Faculty of Medicine and Faculty of Electrical Engineering and Information Technology, Technische Universität München, Troger Straße 32, D-81675 Munich, Germany
[3] Laboratory for Biooptics and Molecular Imaging, Center for Molecular Imaging Research, Massachusetts General Hospital and Harvard Medical School, 149 13th Street, Charlestown, MA 02115, USA
[4] Center for Systems Biology, Massachusetts General Hospital and Harvard Medical School, Richard B. Simches Research Center, 185 Cambridge Street, Boston, MA 02114, USA

E-mail: dr@tum.de

Received 10 November 2008, in final form 8 January 2009
Published 15 April 2009
Online at stacks.iop.org/PMB/54/2769

Abstract

Mesoscopic-scale living organisms (i.e. 1 mm to 1 cm sized) remain largely inaccessible by current optical imaging methods due to intensive light scattering in tissues. Therefore, imaging of many important model organisms, such as insects, fishes, worms and similarly sized biological specimens, is currently limited to embryonic or other transparent stages of development. This makes it difficult to relate embryonic cellular and molecular mechanisms to consequences in organ function and animal behavior in more advanced stages and adults. Herein, we have developed a selective-plane illumination optoacoustic tomography technique for *in vivo* imaging of optically diffusive organisms and tissues. The method is capable of whole-body imaging at depths from the sub-millimeter up to centimeter range with a scalable spatial resolution in the order of magnitude of a few tenths of microns. In contrast to pure optical methods, the spatial resolution here is not determined nor limited by light diffusion; therefore, such performance cannot be achieved by any other optical imaging technology developed so far. The utility of the method is demonstrated on several whole-body models and small-animal extremities.

(Some figures in this article are in colour only in the electronic version)

[5] Author to whom any correspondence should be addressed.

1. Introduction

Spectacular developments of optical microscopy techniques utilizing virtual optical sectioning have resulted in the ability to capture high-resolution three-dimensional (3D) reconstructions of biological specimen *in vivo* (Lichtman and Conchello 2005). Developments in confocal and multi-photon microscopy offer powerful imaging tools that provide insights into morphological, functional and molecular processes within cells and intact organisms, in studying time-dependent gene and protein function, cell motility and evolution of structures and processes. The increasing need for imaging in biology was recently outlined in the *Nature Methods* editorial (Editorial 2007), which calls for collaboration between engineering and genetics communities in finding new tools for high-throughput phenotyping and several other related imaging tasks.

When imaging with light through tissue, photons interfere with cellular interfaces and organelles leading to multiple scattering events within the specimen under investigation. Microscopic techniques, applied to *in vivo* imaging, typically utilize mechanical or physics phenomena to reduce the effect of scattering on image resolution. For example, confocal microscopy (Minsky 1961) employs a pinhole in front of a detector to reject all other photons but the ones that are coming from an in-focus point within the sample. Nonlinear techniques, such as multi-photon microscopy (Denk *et al* 1990) or CARS imaging (Zumbusch *et al* 1999), exploit instead localized nonlinear signal generation due to high-order light–matter interactions to minimize the sensitivity to scattering. These techniques have allowed for powerful insights into dynamic biological phenomena, but suffer from inadequate penetration to less than one transport mean free path length (MFPL) in tissue (Ntziachristos *et al* 2005), i.e. the depth where light becomes severely diffused. Depending on the particular tissue that is being imaged, this limit translates to between 0.3 and 1 mm achievable penetration depth by the latest multi-photon microscopy techniques.

In vivo imaging beyond 1 MFPL could offer an important visualization tool for many areas of biology that involve the study of insects, fish, worms and other small-sized living organisms or organs. Often organisms are selected for biological study because they are optically transparent, at least at a young age, and so they can be imaged under a microscope. Investigations become more challenging as the organism grows and becomes less transparent. Correspondingly, a significant part of *in vivo* biological research revolved so far around the study of organisms that are virtually transparent, such as *Drosophila* larva (Bai *et al* 2008), embryonic (early) stages of zebra-fish (Koster and Fraser 2001) or *Caenorhabditis elegans* (Knobel *et al* 2001) and others. Alternatively, studies are done post-mortem by performing histological sections (Rogulja-Ortmann *et al* 2007). Recently, volumetric optical imaging techniques that account for the diffusive propagation of photons were developed demonstrating whole-body 3D molecular imaging of mice *in vivo* (Graves *et al* 2003). These methods however utilize photon-diffusion theory, which is not suitable for imaging specimens smaller than 1 cm in diameter.

In developing optical projection tomography to image smaller structures, such as embryos, Sharpe *et al* (2002) also noted the need for mesoscopic imaging; however, image complications from scattering were resolved in this case by chemically treating the specimen of interest post-mortem, in order to make the samples transparent. Similarly, selective-plane illumination microscopy (SPIM) (Dodt *et al* 2007) offered high-resolution images of either chemically treated transparent samples or specimens that were smaller than the MFPL.

In order to move beyond the 1 MFPL limit and allow visualization of organisms and structures in the mesoscopic scale, for instance worms, insects or small-animal extremities with optical contrast, we investigated herein the utility of optoacoustic tomography for

whole-body visualization of mesoscopic-scale samples and organisms. Optoacoustics (or photoacoustics) rely on ultrasonic detection of pressure waves generated by the absorption of pulsed light in elastic media (Gusev and Karabutov 1993). The amplitude of the generated broadband ultrasound waves reflects the local optical absorption properties of tissue, whereas the relative timing in the detection of signals can be processed tomographically to determine the volumetric position of the tissue absorbers. As opposed to other light-based imaging methods, in optoacoustics the spatial resolution is not affected by light diffusion but rather by diffusion-free ultrasound propagation; therefore, nearly the same resolution can, in principle, be retained at any detectable imaging depth. Thus, in-depth optoacoustic imaging of diffuse tissues preserves both the reach optical contrast and high (diffraction-limited) ultrasonic resolution. It has already been shown feasible to resolve vascular and other structures in mice and humans (Hoelen *et al* 1998, Kruger *et al* 2003, Wang *et al* 2003), as well as exogenous chromophores and fluorochromes (Li *et al* 2007, Razansky *et al* 2007). Applied in reflectance scanning mode, functional photoacoustic microscopy has also demonstrated the ability for high-resolution imaging of subcutaneous tumor angiogenesis and blood oxygen saturation in rats and humans (Zhang *et al* 2006).

Herein we have developed an optoacoustic tomography scanner based on selective-plane illumination. When combined with confocal detection and specimen rotation over 360° projections, this technology extends imaging into living biological specimens of dimensions never optically visualized in the past. Consequently, we examine for the first time the performance of this method in imaging several important intact model organisms having no hemoglobin-based contrast. The scalability of the technology with different sizes in the mesoscopic scale is also demonstrated.

2. Materials and methods

2.1. Selective-plane optoacoustic tomography setup

The schematic of the experimental setup is shown in figure 1. It utilizes an optical parametric oscillator (OPO)-based laser (MOPO series, Spectra Physics Inc., Mountain View, CA), tunable in the visible and near-infrared region (430–1800 nm). The imaged objects were rotated using a rotation stage, controlled via a stage controller (SC, ESP-3000, Newport Corp., Irvine, CA). The laser beam was focused, using a cylindrically focusing lens, onto the sample submerged into water, thus creating a planar sheet of light (as shown in figures 1(a) and (b)). The focal line was usually extended for about 1 MFPL into the scattering object so as to allow maximal possible confinement of the planar light sheet within the acoustic detection plane (image plane). As many organisms may present particularly high absorption contrast between different structures, this kind of selective-plane illumination strategy is especially useful in the cases studied herein. This is because the light is only partially diffused as it passes through the mesoscopic-scale objects (diameters up to few mm), and thus signals coming from 'out-of-focus plane' absorptive structures are minimized. We estimate that, due to cylindrical focusing, the radiant exposure upon the imaged surface was in the range 20–100 mJ cm^{-2}, depending on the size of the particular object.

Ultrasonic transducers (models V319 and V382, Panametrics) with central frequencies of 15 MHz and 3.7 MHz, respectively, cylindrically focused in the optical illumination plane (confocal arrangement) were used to detect the optoacoustic signals. As shown in figure 1, the detector is located off the laser illumination axis; therefore, no direct illumination of the transducer's surface occurs. The main reasons behind selection of this particular detection configuration are sensitivity and reduction of data acquisition time in order to enable practical

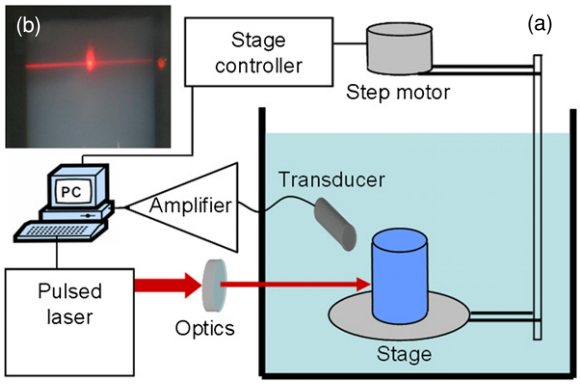

Figure 1. Experimental setup of selective-plane optoacoustic imaging. (a) Schematic of the complete setup; (b) photograph of the cylindrically focused beam passing through agar phantom embedding *Drosophila* pupa.

in vivo imaging applications. Ideally, for high-resolution and quality optoacoustic tomographic reconstructions, the detection bandwidth should be as large as possible. Unfortunately, current ultrawide-band ultrasound detection technologies, such as pVDF film detectors (Razansky and Ntziachristos 2007) and Fabry–Perot interferometric approaches (Zhang *et al* 2008), suffer from low sensitivity and signal-to-noise ratio (SNR) that greatly prolong acquisition times and compromise image quality and contrast, especially in deep-tissue imaging applications, and thus severely limit feasibility and potential application areas. Piezocomposite technology is therefore used due to its generally higher SNR and robustness in exchange, however, for narrow bandwidth. Additionally, acoustic focusing is used here in order to increase detection area and sensitivity, again, in exchange for compromising image quality and resolution along dimensions where focusing is performed.

The recorded time-resolved signals were amplified, digitized and averaged by an embedded oscilloscope PCI card at 100 Msps (NI PCI-5122, National Instruments Corp., Austin, TX) with a 14-bit resolution. The samples were rotated 360° with 3° steps in order to enable in-plane 2D image reconstruction using a filtered backprojection algorithm (Razansky and Ntziachristos 2007). Planar image data acquisition normally took about 2 min while image reconstruction on a dual-core Pentium IV 3.2 GHz processor, having 2 GB RAM, required an additional 5 s.

2.2. Reconstruction of optical absorption using optical projection tomography (OPT) principles

Laser beam from an Ar+ CW laser tuned at 488 nm was focused (beam diameter of about 0.6 mm) in close proximity to the central area of the sample's surface. The imaged pupa was held in place on a holder and rotated along its A/P axis by way of a high-speed rotation stage (Newport, PR50) with an absolute accuracy of 0.05°. Three distinct manual controllers allowed for the pupa's A/P axis to be tilted and adjusted in its orthogonal plane. Light transmitted through the pupa was collected with a Leica microscope consisting of a Z16 APO. An analyzer in front of the microscope selected photons with their polarization parallel to the incident ones, a process which rejected highly diffusive photons (∼10% of the photons collected). The images in this transillumination mode were acquired with a CCD (Pixel Fly QE) with a pixel array of 1392 × 1024 (pixel size 6.5 × 6.5 mum), 12-bit dynamic range,

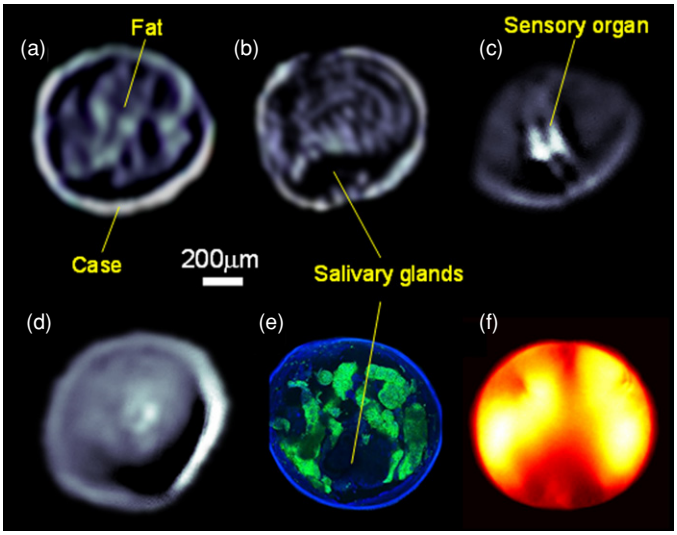

Figure 2. Images of a *Drosophila* pupa. Selective-plane optoacoustic images taken at three different heights: (a) bottom area; (b) salivary gland area; (c) top part containing a dark-color (highly absorbing) sensory organ of the pupa; (d) optoacoustic tomography reconstruction using broad illumination and detection from the salivary gland area; (e) histological section at the salivary gland area (blue—DAPI staining; green—EGFP fluorescence expressed in the fatty structures); (f) planar radon-based reconstruction of optical transillumination (optical projection tomography).

and a quantum efficiency of about 50%. Full rotation over 360° with 2° steps provided a total of 180 projections. A set of fixed and variable neutral density filters allowed to control the amount of light on the sample and to keep it low enough preventing damage to the animal and CCD camera. Optical absorption maps of the imaged object were subsequently reconstructed using filtered radon transform applied to the set of images collected from all the projections.

3. Results

We imaged several model organisms that relate to biological discovery, whose diameter spans the mesoscopic range from 800 μm to 1 cm. Figures 2(a)–(c) show reconstructed images of developing *Drosophila* in its pupal stage using 750 nm selective-plane illumination and a 15 MHz ultrasonic transducer, having a cylindrical focal distance of 19 mm, for detection. The imaging planes were at three different levels—bottom (figure 2(a)), salivary gland area (figure 2(b)) and the top level containing highly absorbing sensory organ of the pupa (figure 2(c)). The corresponding histological section (Vinegoni *et al* 2008) at the salivary gland level is shown in figure 2(e) and shows good agreement with the reconstruction. It must be pointed out that *Drosophila* in its pupal stage is a fairly diffusive organism, not accessible through its intact case by microscopy techniques. By using the herein suggested method, the pupal case is readily identified in figures 2(a) and (b) as having rather high optical absorption as compared to the other structures. The various fatty structures are also clearly visualized with in-plane spatial resolution on the order of 37 μm, limited by the useful bandwidth of the ultrasonic detector (up to 20 MHz). The vertical resolution is determined by the effective focal width of the transducer, i.e. about 100 μm. The area containing the salivary glands is distinguishable in both optoacoustic and histological images, indicating low optical absorption

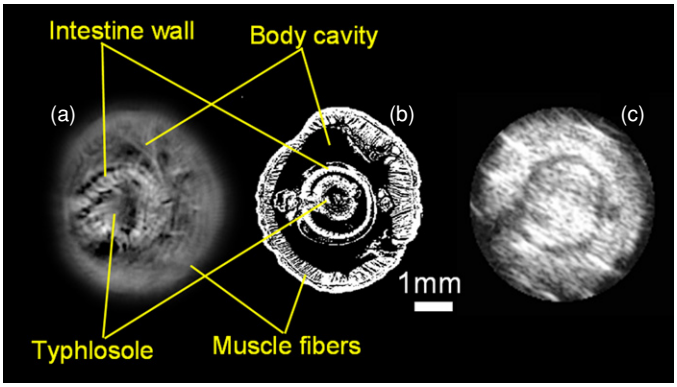

Figure 3. Cross-sectional images of *Lumbricus terrestris* (earthworm) in the intestine area. (a) Selective-plane optoacoustic image; (b) anatomical diagram; (c) the corresponding ultrasound image acquired using a high-resolution ultrasound imaging system operating at 25 MHz.

properties. It is important to emphasize that *Drosophila* organisms, embedded into agar phantoms, remained alive during the short imaging sessions. In order to prove the usefulness of the selective-plane method, we performed the measurement from the salivary gland area, but using wide-beam instead of selective-plane illumination. The resulting image (figure 2(d)) appeared blurred with a reduced contrast. The bright spot in the middle can presumably be related to the black-colored highly absorbing sensory organ of the pupa situated outside the ultrasonic detection plane. Since the whole pupa was illuminated, this sensory organ, although located at a much higher level, produced out-of-plane artifact. In contrast, it is clearly visualized in the selective-plane image acquired from the top area (figure 2(c)). For another comparison, we imaged the pupa using optical transillumination and reconstructed the optical absorption properties with radon transform, i.e. using the optical projection tomography (OPT) technique (as described in Section 2.2 and Sharpe *et al* 2002). The resulting image is shown in figure 2(f). While the low-absorbing salivary gland area is clearly visible in this image, the fatty structures appear with a poor spatial resolution, as expected when imaging through a highly scattering object. Moreover, the latter method is naturally not able to visualize and reconstruct the high-absorption properties of the symmetrically surrounding pupa case.

Figure 3 shows planar images obtained from the intestine area of *Lumbricus terrestris*, also well known as the earthworm. This species is larger in size as compared to *Drosophila* pupae. Although the diameter of an adult worm is usually greater than 3–4 mm, selective-plane optoacoustic imaging proved useful also in this case using the same 15 MHz ultrasonic transducer for detection. The reconstructed image in figure 3(a) provides detailed information about the inner structures (similar to histological section in figure 3(b)), including intestine with the folded structure of its wall, the typhlosole, muscles and dorsal and ventral blood vessels. For comparison, a pure ultrasound image of the same worm, acquired using a high-resolution ultrasound imaging system operating at 25 MHz (VisualSonics Vevo 660^{TM}, VisualSonics Inc., Toronto, Ontario), failed to provide any adequate anatomical information, as evidenced from figure 3(c). It should be noted that the diffusion light theory is poorly applicable to the worm since the MFPL occupies a considerable portion of its radius. Therefore, it is also not accessible by the diffusion optical tomography methods.

In order to demonstrate its wide scalability over different size dimensions, we applied the suggested method for imaging the pelvic limb of a wild-type Balb/c mouse in the interosseous

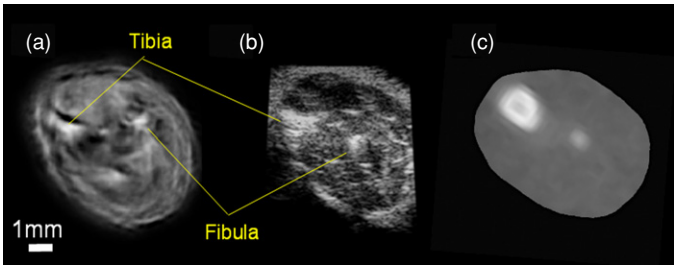

Figure 4. Images obtained from the pelvic limb of a wild-type Balb/c mouse: (a) optoacoustic tomography reconstruction using a 3.7 MHz transducer; (b) the corresponding ultrasound image made with a 25 MHz transducer; (c) the corresponding micro-CT image.

space of the crus area. This is also a mesoscopic object whose characteristic diameter lies in the 5–10 mm range. As was already mentioned, highly sensitive focused piezocomposite detectors used in our study provided limited bandwidth, thus imposing resolution limitations. In addition, focusing created an interplay between lateral (in-plane) and vertical (focal-width-limited) resolutions, causing scaling problems since it was no longer possible to image objects with different sizes and spatial frequency variations using the same detector. For smaller objects and the corresponding regions of interests, like pupa and worm, that were imaged with the 15 MHz transducer, it was possible to bring the detector's focus in closer vicinity of the imaged area, which thus reduced problems associated with acoustic dispersion and increased attenuation of high-frequency ultrasound components (Razansky *et al* 2009). This allowed tighter focusing and improved lateral and vertical resolution. On the other hand, the resolution was given up and a different detector and focusing configuration were used when imaging larger regions of interest. In the case of mouse leg, the imaging target had an elliptic-like cross-section of about 10 mm by 7 mm in the imaging plane. Therefore, due to the relatively large size of the object, we used a 3.7 MHz transducer with a cylindrical focal distance of 38 mm. The in-plane resolution in this case was set by 5 MHz useful bandwidth to about 150 μm and the focal width, determining the vertical resolution, was about 1 mm.

The reconstructed planar optoacoustic image is presented in figure 4(a) along with the corresponding ultrasonic (figure 4(b)) and micro-CT (figure 4(c)) images, acquired approximately at the same imaging plane with the high-resolution ultrasound imaging system (figure 4(b)). Evidently, the triangular *tibia* and the *fibula* bones are clearly visualized by all the three modalities. However, one may note that the optoacoustic image, although acquired by a much lower frequency transducer, provides enhanced contrast and other fine details that are not available in the ultrasound or CT images.

4. Discussion

The ability to optically interrogate and visualize intact organisms is of high importance due to the great variety of intrinsic optical contrast and exogenous molecular probes available in the visible and near-infrared spectra. In this work, a selective-plane illumination optoacoustic tomography technique was developed and applied for high-resolution whole-body visualization of intact mesoscopic-scale optically diffusive organisms whose sizes may vary from sub-millimeter up to a centimeter range. The size of many relevant biological samples and model organisms, e.g. developing insects, small-animal extremities, animal and fish embryos as well as embryos of some adult fishes, lie in this range. However, due to the high optical diffusion and relatively small size, they are not accessible by existing optical

microscopy nor by diffusion-based optical tomography methods like fluorescence molecular tomography (Graves *et al* 2003, Ntziachristos *et al* 2005). Thus, selective-plane optoacoustic imaging holds promise of becoming the method of choice for imaging those organisms. Although it is known that optoacoustic imaging is sensitive to hemoglobin, good contrast was demonstrated herein also for other biological tissues like fat, bones and other internal structures. By applying multispectral optoacoustic imaging (Razansky *et al* 2007), other molecularly relevant information contained in the optical spectrum can potentially be resolved, for instance fluorogenic or chromogenic bio-markers associated with gene expression, morphogenesis or decease progression.

Several potential hurdles have to be addressed before wide applicability of the method for *in vivo* imaging becomes feasible. First is the requirement for aqueous environment. Although some of the organisms or body parts can be kept alive under water for certain amount of time, imaging of many other targets may still be quite challenging and require complicated setups. The issue of laser safety levels needs further study. The exposure in our study exceeded in some cases the permissible human skin exposure limit for pulsed lasers that is set at 25 mJ cm^{-2} for 750 nm (ANSI 2000). Clearly, the intensities needed for reasonable SNR can be greatly reduced in the future by improving detection sensitivity, reducing noise and making other hardware improvements. However, it is also clear that, as opposed to well-accepted human radiation safety standards, many mesoscopic targets and organisms of interest currently do not have any exposure standards set for *in vivo* imaging using nanosecond lasers that would establish short- and long-term effects and safe intensity levels. Nevertheless, we have noticed that no apparent damage was caused to the imaged objects in our current study.

Overall, we have identified selective plane optoacoustic imaging as a highly promising method in biological discovery. When applying pure optical imaging to diffuse tissues, the spatial resolution is always exchanged for penetration. Therefore, as the size of the imaged object grows, imaging resolution quickly deteriorates (Vinegoni *et al* 2008). It is even possible to perform optical tomography through entire mice with high sensitivity, but a low resolution of about 1 mm or worse (Graves *et al* 2003, Ntziachristos *et al* 2005). In contrast, selective-plane optoacoustic imaging offers a platform for mesoscopic imaging with a resolution that can practically become on the order of 20 μm and less with improved detection technology. In contrast to pure optical imaging, the spatial resolution here is not limited by light diffusion but by the useful bandwidth of the ultrasonic detector, which can be further improved over time to attain better performance. Therefore, no fundamental limitation is imposed on the resolution, which can in principle remain constant for the entire penetration range of several millimeters to centimeter of tissue. Yet, one has to keep in mind that biological tissues introduce ultrasonic dispersion with higher sound absorption at higher frequencies. It is therefore a matter of signal-to-noise ratio that determines which part of the detected spectrum is situated above the noise floor and can be recovered (Razansky *et al* 2009). If the SNR is high enough, effects of ultrasonic dispersion can generally be reversed by spectrally emphasizing higher frequencies. Consequently, if spatial resolution is to be increased by increasing the detection bandwidth, this has to be accompanied by improved sensitivity of acoustic detection or the overall SNR, especially at the higher frequency end.

In conclusion, we demonstrated that, using the developed technique, non-invasive optical imaging during embryogenesis can be extended into opaque and adult stages in many model organisms and tissues. This could in turn open novel venues in numerous fields of genetic research, e.g. investigation of molecular and cellular mechanisms of disease etiology and progression, tumorigenesis and metastasis formation or aging. We currently foresee the application of the method as a guiding strategy toward identification of appropriate time points during development and evolution of organisms scanned non-invasively, on which to euthanize

and perform traditional histological analysis on the specimen of choice. By developing more imaging applications around this technology however, it might also be possible to operate it as a stand-alone modality, to follow dynamic changes over time, in unperturbed environments.

References

American National Standards Institute 2000 American National Standard for the Safe Use of Lasers in Health Care Facilities *Standard Z136.1-2000* (New York: ANSI)

Bai J, Binari R, Ni J-Q, Vijayakanthan M, Li H-S and Perrimon N 2008 RNA interference screening in *Drosophila* primary muscle cells for genes involved in muscle assembly and maintenance *Development* **135** 1439–49

Denk W, Strickler J H and Webb W W 1990 2-photon laser scanning fluorescence microscopy *Science* **248** 73

Dodt H U *et al* 2007 Ultramicroscopy: three-dimensional visualization of neuronal networks in the whole mouse brain *Nat. Methods* **4** 331–6

Editorial 2007 Geneticist seeks engineer: must like flies and worms *Nat. Methods* **4** 463

Graves E E, Ripoll J, Weissleder R and Ntziachristos V 2003 A submillimeter resolution fluorescence molecular imaging system for small animal imaging *Med. Phys.* **30** 901–11

Gusev V E and Karabutov A A 1993 *Laser Optoacoustics* (New York: AIP)

Hoelen C G A, de Mul F F M, Pongers R and Dekker A 1998 Three-dimensional photoacoustic imaging of blood vessels in tissue *Opt. Lett.* **23** 648–50

Knobel K M, Davis W S, Jorgensen E M and Bastiani M J 2001 UNC-119 suppresses axon branching in *C. elegans* *Development* **128** 4079–92

Koster R W and Fraser S E 2001 Tracing transgene expression in living zebrafish embryos *Dev. Biol.* **233** 329–46

Kruger R A, Kiser W L, Reinecke R, Kruger G A and Miller K D 2003 Thermoacoustic molecular imaging of small animals *Mol. Imaging* **2** 113–23

Li L, Zemp R, Lungu G, Stoica G and Wang L V 2007 Photoacoustic imaging of lacZ gene expression *in vivo J. Biomed. Opt.* **12** 020504

Lichtman J W and Conchello J A 2005 Fluorescence microscopy *Nat. Methods* **2** 910

Minsky M 1961 *US Patent Specification* 3,013,467

Ntziachristos V, Ripoll J, Wang L V and Weissleder R 2005 Looking and listening to light: the evolution of whole-body photonic imaging *Nat. Biotechnol.* **23** 313

Razansky D, Baeten J and Ntziachristos V 2009 Detection sensitivity of multi-spectral optoacoustic tomography (MSOT) *Med. Phys.* **36** 939–45

Razansky D and Ntziachristos V 2007 Hybrid photo-acoustic fluorescence molecular tomography using finite-element-based inversion *Med. Phys.* **34** 4293–301

Razansky D, Vinegoni C and Ntziachristos V 2007 Multispectral photoacoustic imaging of fluorochromes in small animals *Opt. Lett.* **32** 2891–3

Rogulja-Ortmann A, Lüer K, Seibert J, Rickert C and Technau G M 2007 Programmed cell death in the embryonic central nervous system of *Drosophila melanogaster Development* **134** 105–16

Sharpe J *et al* 2002 Optical projection tomography as a tool for 3D microscopy and gene expression studies *Science* **296** 541

Vinegoni C, Pitsouli C, Razansky D, Perrimon N and Ntziachristos V 2008 *In vivo* imaging of *Drosophila* melanogaster pupae with mesoscopic fluorescence tomography *Nat. Methods* **5** 45–7

Wang X, Pang Y, Ku G, Xie X, Stoica G and Wang L V 2003 Noninvasive laser-induced photoacoustic tomography for structural and functional *in vivo* imaging of the brain *Nat. Biotechnol.* **21** 803–6

Zhang E Z, Laufer J, Pedley R B and Beard P 2008 3D photoacoustic imaging system for *in vivo* studies of small animal models *Proc. SPIE* **6856** 68560P

Zhang H F, Maslov K, Stoica G and Wang L V 2006 Functional photoacoustic microscopy for high-resolution and noninvasive *in vivo* imaging *Nat. Biotechnol.* **24** 848–51

Zumbusch A, Holtom G R and Xie X S 1999 Three-dimensional vibrational imaging by coherent anti-Stokes Raman scattering *Phys. Rev. Lett.* **82** 4142–5